Packing of semiflexible polymers into viral capsid in crowded environments

N. Al-Naamani and I. Ali*
Department of Physics, College of Science, P.O. Box 36, Sultan Qaboos University, Al-Khod 123, Oman

(Received 17 December 2018; revised manuscript received 26 August 2019; published 26 November 2019)

We use coarse-grained Langevin dynamics simulations to study packing of semiflexible polymers into a spherical capsid, with and without a tail, inside a crowded cell. We use neutral and charged, but highly screened, polymers and compare packing rates of the two. Such packing conditions are relevant, for example, to λ DNA packing inside *Escherichia coli* bacterial cells, where the crowd particles are proteins, bacterial DNA, and salts. For a neutral polymer packing into a capsid with a tail, attractive interactions with the crowd particles make packing slightly harder at higher crowd densities, but repulsive interactions make it easier. Our results indicate that packing into a tailless capsid is less efficient at low crowd densities than into one with a long tail. However, this trend becomes opposite at higher densities. In addition, packing into a capsid with a long tail shows a highly variable waiting time before packing initiates, a feature absent for a tailless capsid. Electrical interactions at physiological conditions do not have much effect. Some bacterial cells, such as *Pseudomonas chlororaphis*, form a nucleuslike structure encapsulating the phage 201ϕ2-1 DNA. We also study here the packing dynamics with the nucleus present. We find packing is faster compared to the case of no-nucleus packing. We also observe knot formations but these knots untangle quickly while the polymer translocates. This knot formation is independent of polymer charge and presence of crowd particles.

DOI: 10.1103/PhysRevE.100.052412

I. INTRODUCTION

Packing of the DNA genome into a bacteriophage is an important stage in the phage life cycle. Extensive studies have been done to understand this process experimentally, theoretically, and computationally [1–10] on different phages. Genome packing in phage λ has been particularly investigated because of its importance in genetic engineering. It is the best vector for the first step in cloning genes. It has high transformation efficiency *in vitro* packing of recombinant DNA into the λ heads and it is used in gene therapy [11].

Experiments demonstrate that packing the DNA into a bacteriophage requires high motor force, reaching tens of piconewtons [1,12,13]. It can, however, exceed 100 pN as is the case with ϕ29 phage [14] due to repulsive DNA-DNA interactions, unfavorable bending of DNA inside the capsid, and entropic penalties. Packing a λ genome takes 120 s on average [13]. During packing, pauses and slips are observed, especially at high forces, and the packing rate decreases as the prohead is filled [1,12–14]. Typically, the packing rate is constant until about 50% of the DNA is packed, decreasing to zero at full packing [1,12–14]. Packing a long DNA into a capsid of dimensions of the order of DNA persistence length ∼50 nm, in addition to electric repulsion among the various DNA sections, causes high capsid internal forces, which are used to initiate ejection of the DNA from the capsid to the bacterial cell during infection. Experiments find that this packed DNA takes a coaxial spool shape [15,16]. However, at lower motor force, the organization of the packed DNA inside the capsid is highly ordered, resulting in smoother exit and few intermediate slow kinetics, hence fewer pauses [17].

Recent experiments show that packing velocity varies from 700 to 320 bp/s for T4 phage [12] and from 600 to 240 bp/s for λ phage [13], depending on the applied load. On the other hand, the packing process is reversible, where it is found, for example, that one-third of T3 genome can exit the capsid into the solution [18]. The maximum limit on the length of DNA that can be packaged into a lambda capsid is slightly above the wild-type genome [19], suggesting that adding more DNA would make the capsid unstable.

Recently, fluorescence microscopy and cryoelectron tomography have been used to study the infection cycle of phage 201ϕ2-1 in *Pseudomonas chlororaphis* cell [20]. It is observed that a nucleuslike structure assembles around the ejected viral DNA. This structure provides a protective environment for DNA replication to proceed. There are proteins inside the compartment, for the DNA replication and transcription, and outside the compartment, for translation and nucleotide synthesis. The viral capsid assembles on the cytoplasmic membrane and then segregates and attaches to the nucleus structure to pack the newly formed DNA. After the capsid is filled with DNA, a tail is attached to it to complete its assembly to form a mature phage [20].

Simulations have tackled many different facets of packing, looking into effects of chain stiffness [21], capsid shape and nonequilibrium effects [22,23], temperature, capsid tail [24], and the presence of ions [25]. These studies point out the importance of fluctuations in the packing process and find that random pauses do occur, becoming longer close to full packing. DNA becomes more ordered if packed inside an elongated capsid and with more DNA self-interaction [23]. DNA self-interaction, in particular, is mediated by the

*Corresponding author: issam.squ.edu.om

presence of multivalent cations, which screen the DNA charge. Larger screening results in larger packing speed [25].

Other studies [26] suggest that the packing process is stochastic in nature and therefore the packed DNA structure does not have to be an inverse spool. As the capsid is filled, the structure, the energy, and packing velocity depend on the polymer dynamics. In addition, work done by Locker *et al.* [27] showed that the packing of T7 genome is coaxial, while the packing of $\phi 29$ genome is concentric. This might be related to the inner cylindrical core structure in the T7 phage that can play a major role in the configuration of the packed genome [28].

Theoretical studies [29] have looked at elastic and electrostatic contributions during double-stranded DNA (dsDNA) packing and ejection. As the DNA is packed, the interstrand space decreases, which increases the resistive force that arises from the bending of the semiflexible dsDNA, entropy, and the DNA-DNA repulsive electrostatic interactions.

In real life, packing a viral DNA occurs inside the bacterial cell, where the environment is crowded due to the presence of proteins, ribosomes, bacterial DNA, and salts. It is expected that crowding particles and cellular confinement would affect packing efficiency due to various interactions of these particles with the viral DNA, in addition to entropic penalties imposed by confinement.

The aim of this study is to use molecular dynamics–based simulations to study the packing of a coarse-grained semiflexible polymer into a spherical capsid (with and without a long tail). We specifically look at the effects of crowding density, interaction of crowding particles with the polymer, the presence of the capsid tail, and the effects of electrical interactions of crowding particles with the polymer.

We find that a tailless capsid is more efficient at packing at densities used in this study. In addition, electrical interactions can either aid or slow packing, depending on whether they are repulsive or attractive, but their effect is small.

As mentioned earlier, *P. chlororaphis* forms a nucleuslike structure encapsulating the $201\phi 2$-1 phage DNA [20]. We also study this case and find that encapsulating a polymer makes its packing faster compared to the case where no nucleus is present. We also find that the polymer forms knots while being packed.

The paper is organized as follows: Section II details our simulation model, followed by results and discussion in Sec. III. We conclude in Sec. IV.

II. SIMULATION MODEL

We use coarse-grained Langevin dynamics simulations, within the framework of LAMMPS [30], which is a very efficient molecular dynamics code and is freely available, to model the viral capsid, the bacterial wall, the viral DNA, the bacterial proteins, and the nucleus structure. We give the model details in the sections below (see also Fig. 1).

A. Double-stranded DNA

The viral DNA is coarse-grained into beads, each of diameter σ ($\sigma = 2.5$ nm, width of DNA base pair). These beads are connected by finite extension nonlinear elastic (FENE) springs. The total length of λ DNA is around 16.5 μm [13]. However, to make the size of the system manageable for computational time, we shrink the length by a factor of 16. Thus we coarse-grain the DNA to 400 beads (a contour length of about 1 μm = 2.9 kbp).

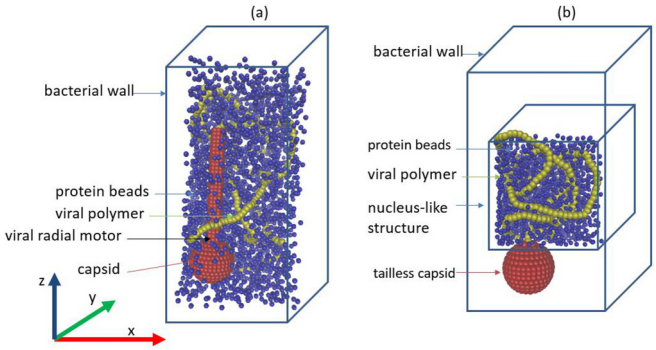

FIG. 1. (a) Coarse-grained model of spherical capsid with a tail, dsDNA, proteins, and cell wall at the initial state of equilibration. (b) Coarse-grained model of spherical tailless capsid, dsDNA, proteins, nucleus-structure wall, and cell wall at the initial state of equilibration.

We also include the bacterial DNA in some of our simulations. The bacterial DNA for *Escherichia coli* is about 5.5 Mbp [31] (about 1870 μm). However, we shrink its size to 2800 beads (about 7 μm), to maintain stability of the simulations, and break it to 7 polymers each of 400 beads length (packing occurs in nature when the bacterial DNA in *E. coli* is broken [32]).

The FENE potential connecting two consecutive beads is

$$U_{\mathrm{FENE}}(r_{i,i+1}) = -0.5kR_0^2 \ln\left[1 - \left(\frac{r_{i,i+1}}{R_0}\right)^2\right]. \quad (1)$$

It is an attractive potential with maximum bond extension of $R_0 = 1.5\sigma$ [33,34]. We set the bond energy $k = 30\epsilon/\sigma^2$. The distance between the ith bead and $(i+1)$st bead is $r_{i,i+1}$. We add a repulsive interaction for excluded volume using the Lennard-Jones (LJ) potential,

$$U_{\mathrm{LJ}}(r_{ij}) = 4\epsilon\left[\left(\frac{\sigma}{r_{ij}}\right)^{12} - \left(\frac{\sigma}{r_{ij}}\right)^{6}\right] + \epsilon, \quad (2)$$

where r_{ij} is the distance between the ith and jth beads with a cutoff at $2^{1/6}\sigma$, the minimum of the LJ potential and $\epsilon = k_BT$ (k_B is the Boltzmann constant) in our simulations. A real DNA has persistence length of ∼50 nm, which we mimic by applying a stiffness potential U_θ,

$$U_\theta = K_\theta(1 + \cos\theta), \quad (3)$$

where θ is the angle between three consecutive beads along the chain. $K_\theta = 20\epsilon\sigma$ is the force constant (bending modulus [35]) for the angular stiffness. It determines the persistence length l_B, where $l_B = K_\theta/\epsilon = 20\sigma = 50$ nm.

In real life, DNA has negative charge due to the phosphate group. We compare here the packing of a charged polymer with that of a neutral one. The electrostatic interaction between the DNA beads is modeled using the Debye-Huckel

potential $U_{\rm DH}$,

$$U_{\rm DH}(r_{ij}) = C\left(\frac{q_i q_j}{\epsilon_r}\right)\left(\frac{e^{\kappa a}}{1+\kappa a}\right)\left(\frac{e^{-\kappa r_{i,i+1}}}{r_{i,i+1}}\right), \qquad (4)$$

where $C = (\frac{1}{4\pi\epsilon_0 k_B T})$, q_i is the charge of the ith bead, ϵ_r is the dimensionless dielectric constant (we consider $\epsilon_r = \epsilon_{\rm water} = 80$), κ is the inverse Debye length, and a is the bead's radius. For water at 37 °C, κ^{-1} is 1.87 nm and $k_B T = 4.3$ pN nm at 37 °C.

DNA charge is highly screened due to the presence of multivalent ions in bacterial cells. We set $\kappa = 2.5/\sigma$, corresponding to a screening length of 1.0 nm [36]. In addition, each base pair carries a charge of $-2e$, due to the negatively charged phosphate group. Each DNA bead in our model, however, is equivalent to 7.4 bp. Considering that the phosphate groups in the DNA are typically neutralized at the level of 80%–100%, we set the charge of the DNA bead 80% lower to $-2.96e$.

B. Capsid, tail, and viral motor

The phage is modeled as a spherical capsid of outer diameter 10σ. The capsid is centered in the middle of the cubic simulation box. Our capsid is formed from 585 beads, each bead having a diameter of σ. We remove some beads at the topmost location of the sphere to form a hole of diameter 1.7σ, thus permitting the entry of one viral DNA bead at a time. The capsid beads interact with the viral polymer and protein beads (see Sec. II C below) via the LJ potential.

We obtain a polymer packing fraction of 40% with our capsid. The packing density in our simulations becomes 55% if we use the internal capsid diameter of 9σ, close to other calculations. (If we take into account the fact that the LJ potential does allow for interacting beads to penetrate slightly into each other, at the level of $\sim 0.1\sigma$, then our packing fraction is about 50%).

In terms of genome packing fraction, our 400-beads polymer corresponds to 2.9 kbp, as mentioned above. This results in an apparent packing fraction of 0.34 bp/nm^3, which is lower than reported by Earnshaw and Casjens [37]. However, if we use the internal capsid diameter of $9\sigma = 22.5$ nm, then we obtain a fraction of 0.49 bp/nm^3. This latter value is consistent with, and slightly higher than, 0.507 calculated by Purohit *et al.* [29], who have used the capsid's internal volume to find the distance between DNA strands as a function of DNA fraction packed in various phages, based on *in vitro* experiments.

Although our model results in a capsid diameter of 25 nm, which is less than the λ phage diameter of ∼55 nm, it still gives conditions that are relevant to experiments. For example, the packing rate for this capsid decreases as the capsid is filled with our polymer, similar to experimental observations [1].

To model the tail, we add extra beads to form a long hollow cylinder at the top of the capsid hole. The internal diameter of the cylinder is 1.7σ and its length is $\sim 27\sigma$, which is three times the length of the capsid diameter (as in λ phage). The forces on the capsid and the tail beads are zeroed so they remain at the rest.

The capsid motor feeds the beads into the capsid during packing. Experiments on $\phi 29$ phage have found that different ions can affect motor packing speed [38]. However, these experiments are performed under controlled conditions where charge concentrations can be varied at will, which is not the case for a bacterial cell environment. Furthermore, the motor itself is a rather complex structure. Therefore, and for simplicity, we model the motor as a radial constant force at the capsid hole. It feeds the viral polymer beads towards the center of the capsid. The force is set to 80 simulation units, corresponding to 128 pN, which is approximately the minimum force needed to pack the polymer when the volume fraction of crowding particles in the bacterial cell is 10% (the maximum volume fraction used in this study and where packing is most difficult). Whether the capsid has a tail or not, the location of the motor remains the same at the topmost location of the spherical capsid.

C. Bacterial wall and nucleuslike structure

In real life the bacterial DNA packing fraction is 0.15-0.25 for the *E. coli* bacterial cell [39]. The cell itself is approximately $1000 \times 1000 \times 2000$ nm^3. We shrink each dimension by a factor of 14 and our bacterial cell is a rectangle of dimensions $29 \times 29 \times 58\sigma^3$.

P. chlororaphis phage $201\phi 2$-1, on the other hand, forms a nucleus at the cell's center, enclosing the phage DNA [20]. Packing occurs from this nucleus into a tailless capsid in the center of the cell. We model the shell as a cube of length 22σ (which is about one-quarter the size of the cell as estimated from the figures of Ref. [20]) and attach our capsid to its surface. It is unknown so far whether *E. coli* forms such a structure. This enables us to compare results with and without the nucleus present.

Each cellular and nuclear wall generates a hard repulsive force perpendicular to itself and to any bead coming within a distance 1.122σ of the wall. In LAMMPS, this force is derived from the potential

$$U_{\rm wall} = \epsilon\left[\frac{12}{5}\left(\frac{\sigma}{r}\right)^9 - \left(\frac{\sigma}{r}\right)^3\right], \qquad r < 1.122\sigma. \qquad (5)$$

D. Proteins

Proteins are modeled as nonbonded beads where the diameter of each bead is σ. We use the Lennard-Jones potential to describe the interaction among all interacting beads (proteins, DNA, and capsid) [see Eq. (2)].

In this study we look at the effect of proteins on the viral DNA packing. So we initially set the protein bead–DNA bead interaction as repulsive ($r_{\rm cut} = 1.122\sigma$) and then we compare it to when the interaction is attractive ($r_{\rm cut} = 2.5\sigma$). In both cases, protein-protein, protein-capsid, and DNA-capsid interactions are repulsive ($r_{\rm cut} = 1.122\sigma$).

In order to study the effects of electrical interactions, we also use the Debye-Huckel potential to describe the interaction between any two interacting protein-protein and protein-DNA beads. For simplification, we consider the same magnitude of charge q for the polymer and protein beads, as we are currently interested only in gross effects of various parameters.

E. Fluid inside the bacterial cell

To account for the effects of the viscous medium inside the bacterial cell, the force fields on each bead are computed by simulating the Langevin equation in LAMMPS [30],

$$m_i \frac{d^2 r_{ij}}{dt^2} = -\nabla_j U_i + f_{ij} - \gamma_i \frac{dr_{ij}}{dt} + F_{ij}, \tag{6}$$

where m_i is mass of the ith bead, r_{ij} is the jth component of its position vector, U_i is the net potential acting on it, and t is time. γ_i is the friction coefficient of the ith bead, f_{ij} is the jth component of the random force acting on it, whose magnitude is $\sqrt{2k_BT\gamma_i\delta t}$ (in terms of the simulation time unit τ, $\delta t = 0.01\tau$ is the simulation time step for all simulations, except for the ones involving the nucleuslike structure, where $\delta t = 0.001\tau$). $\gamma = 7.5 \times 10^{-13}$ Ns/m for a sphere of diameter 2.5 nm in water [26]. The timescale τ is determined from the fluctuation-dissipation theorem [26], where $\tau = 6l_{\text{sim}}^2\gamma/k_BT \sim 20\ \mu$s for our study. F_{ij} is the motor force on the ith bead.

The net potential acting on bead i is the sum of all the nonbonded and bonded interactions, Eqs. (1)–(5):

$$U_i = U_{\text{FENE}i} + U_{\text{LJ}i} + U_{\theta i} + U_{\text{wall}i} + U_{\text{DH}i}. \tag{7}$$

The Langevin dynamics simulation proceeds through solving the equations of motion of N particles where the net force on each bead is $= -\nabla U$. The velocities and positions are updated using the standard velocity Verlet algorithm [40].

III. RESULTS AND DISCUSSIONS

Our system size is smaller than that found in nature (for example, as mentioned above, our viral DNA is 1 μm in length, about 16 times smaller than the natural λ DNA length). Our main aim here is to study the gross effects on DNA packing, which is significantly affected by crowding particles volume fraction and the DNA packing density inside the viral capsid. Other simulation studies [22,26] that use smaller systems have found results that qualitatively agree with experiments, for example, the packing rate decreasing as the capsid is filled with the viral polymer [1] and that the capsid force on the packed DNA deceases due to DNA relaxation inside the phage [41].

For each simulation run, we randomly configure and equilibrate the protein and viral DNA beads inside the bacterial cell. We leave two beads of the viral polymer inside the capsid during equilibration. The packing force is turned on after equilibration. We also randomly configure and equilibrate the seven bacterial DNA polymers. We perform additional simulations where packing occurs *in vitro* (bacterial cell, bacterial DNA, and proteins removed from our simulations) to facilitate a comparison with current experimental conditions.

We consider packing inside an empty cell, a cell filled with 3000 beads (mimicking proteins at 5% packing fraction), a cell filled with 6000 beads (proteins at 10% volume fraction), and a cell containing 3000 protein beads with seven 400-beads-long bacterial polymers (also 10% volume fraction).

As mentioned above, the phage 201ϕ2-1 forms a nucleus encapsulating the phage DNA. Lacking any further experimental data, we assume the protein volume fraction inside this nucleus to be the same as that of the cell. So we randomly fill and equilibrate the nucleus in our simulations with 1017 (5% volume fraction) and then with 2070 (10% volume fraction) charged beads.

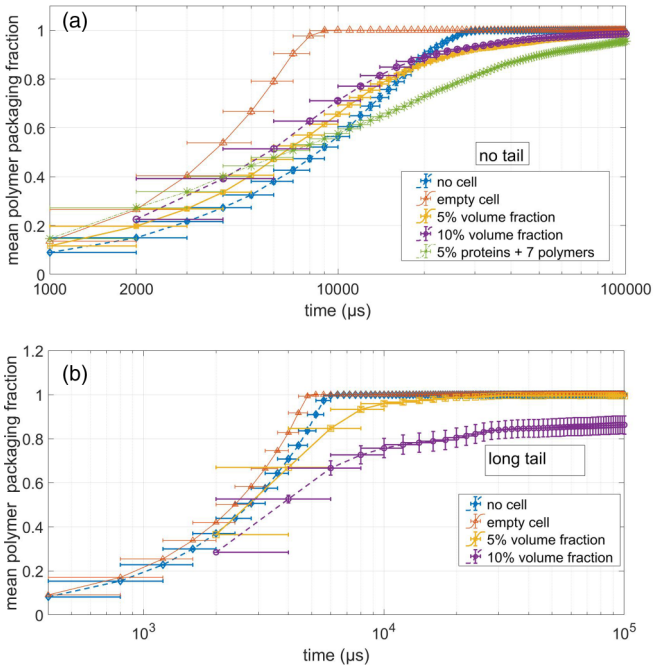

FIG. 2. (a) The mean polymer length packing fraction in the capsid with no tail versus time during polymer packing *in vitro*, inside an empty cell, and a cell containing 3000 proteins (5% volume fraction) and 6000 proteins (10% volume fraction). Interactions among all beads are repulsive. (b) Same as (a) but for a capsid with a long tail (three times the capsid diameter).

A. Effect of crowded environment

No known phage has ever been observed to pack its DNA through its tail. Nevertheless, it is interesting, from a fundamental point of view, to compare packing with a capsid with a tail (Fig. 2). We plot the mean polymer length packaged versus time averaged over 43 to 100 runs for packing *in vitro*, inside an empty cell, a cell containing 3000 beads (5% volume fraction), and a cell containing 6000 beads (10% volume fraction). All interactions are repulsive.

We find that, irrespective of tail, packing inside an empty cell is faster than packing *in vitro*. Our polymer is highly confined in the cell [its end-to-end distance, with error on the mean $\leqslant 10\%$, shrinks from 73σ *in vitro* to 48σ inside the empty cell, with its projection on the x-y plane (see Fig. 1) reducing from 37σ to 11σ]. The polymer has larger possibilities *in vitro* to adopt different configurations allowing it to fluctuate more, making it harder for the beads to be inserted in the capsid hole. However, inside the cell, the viral polymer suffers entropic loss and this makes it easier to package the polymer due to the reduction in fluctuations.

Adding crowding particles slows down packing. As the number of protein beads increases, the packing time increases because the repulsive interactions among protein and viral polymer beads contribute additional resistive (friction) force that lowers packing speed. Additionally, the polymer is even

more compact with crowd particles present [its end-to-end distance is about $(20 \pm 1)\sigma$] due to depletion forces [42]. This makes it unfavorable for the polymer to extend in order to pack, further contributing to packing slowdown. Moreover, we see stalling events at high protein beads density (10% volume fraction), when packing into a capsid with a tail, where packing speed slows down rapidly when 60%–70% of the polymer is inside the capsid.

Keeping the volume fraction constant at 10%, we compare packing with 6000 protein beads present to that with 3000 beads plus seven 400-beads-long semiflexible polymers, to mimic the broken bacterial DNA. In the latter case, the fact that about 2800 are connected into polymers clearly slows down packing even further, as seen in Fig. 2(a). This is because the viral polymer has to move around these polymers before being able to bring its beads to the capsid entrance.

Looking at Fig. 2(a) in closer detail, we find that the packing speed throughout the packing process for the case of 5% protein volume fractions is, within the statistics of our study, very similar to the case of 10% protein volume fraction. This situation remains the same at early times ($\lesssim 10\,000$ μs) when we include the seven bacterial polymers. However, at longer times, the packing speed in the latter case clearly slows down as the viral polymer tries to find its way around these bacterial polymers. On the other hand, the packing speed is largest when the bacterial cell is empty. This is especially clear at times $\gtrsim$4000 μs. Packing speed *in vitro* seems to be slowest at shorter times, as the motor competes with the viral polymer entropy outside the capsid. Once enough of the polymer is inside, the packing speed increases, resulting in a faster packing time compared to the cases where we have protein beads.

If we attach a tail to the capsid [Fig. 2(b)], then the packing speed throughout the packing process for the empty-cell case

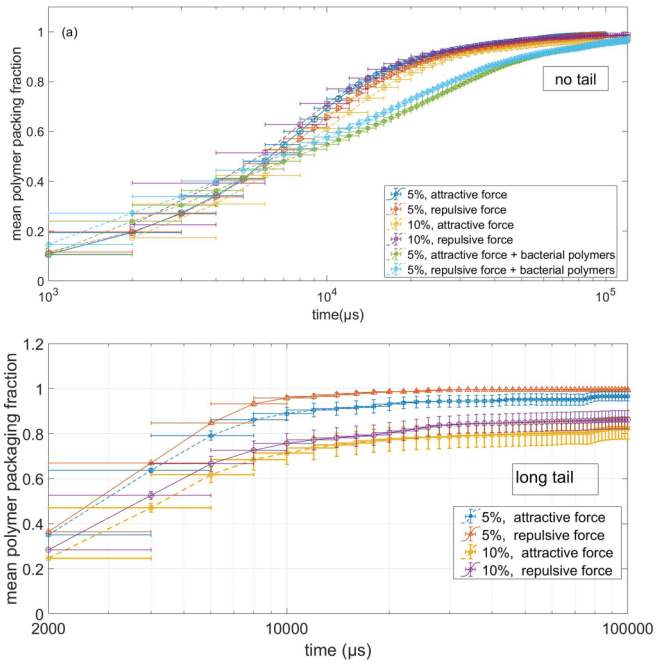

FIG. 3. Effect of attractive force on packing: (a) Capsid with no tail. (b) Capsid with a long tail. Protein volume fractions are indicated in the figures.

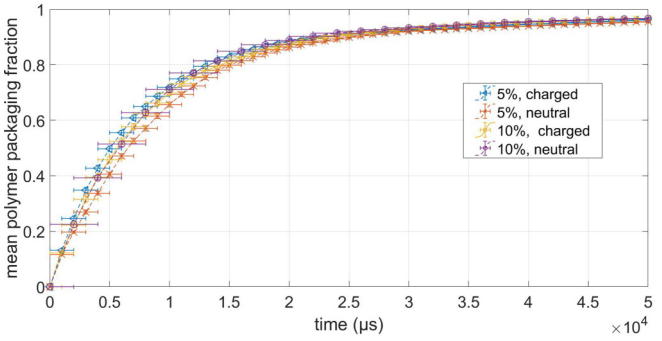

FIG. 4. The mean polymer packing fraction in a capsid with no tail versus time inside a crowded cell. Protein volume fractions are indicated in the figure.

is no different than the no-cell case. The tail significantly reduces the viral polymer entropy. Adding extra confinement in the form of a bacterial cell does not add much extra entropic penalty. Adding protein beads, however, clearly affects the packing speed, where it is slowest at 10% protein volume fraction. This slowness is helped by the opposing capsid pressure and resistive friction provided by the protein beads to the viral polymer.

B. Effect of attractive and electrical force

Figure 3 shows the effects of forces on the packing dynamics. Figure 3(a) is a plot of average polymer length packaged in tailless capsid (average over 40–90 simulation runs) versus packing time. When the bead volume fraction is 10%, we see that attractive forces between the viral polymer and protein beads slightly increase the packing time because the protein beads pull the polymer away from the capsid. This agrees with the idea that binding proteins to the DNA can help in pulling the genome as argued by Molineux that ejecting the DNA into the cell is assisted by the DNA binding proteins [43]. However, the nature of the forces (attractive versus repulsive) does not have much effect on the packing rate at 5% protein volume fraction. We also see this when we add the seven bacterial polymers in our simulations, indicating that the dynamics is mostly controlled by the viral polymer finding its way around the bacterial polymers in order to pack. For

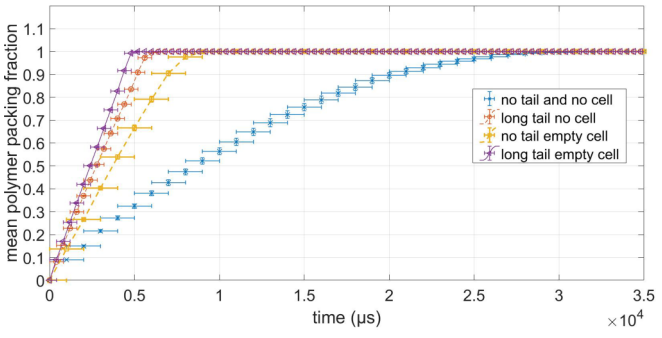

FIG. 5. Comparison of polymer packing into a capsid *in vitro* with that of a capsid inside an empty cell. The plot shows the mean polymer length packaged vs time for a capsid with no tail and one with a tail.

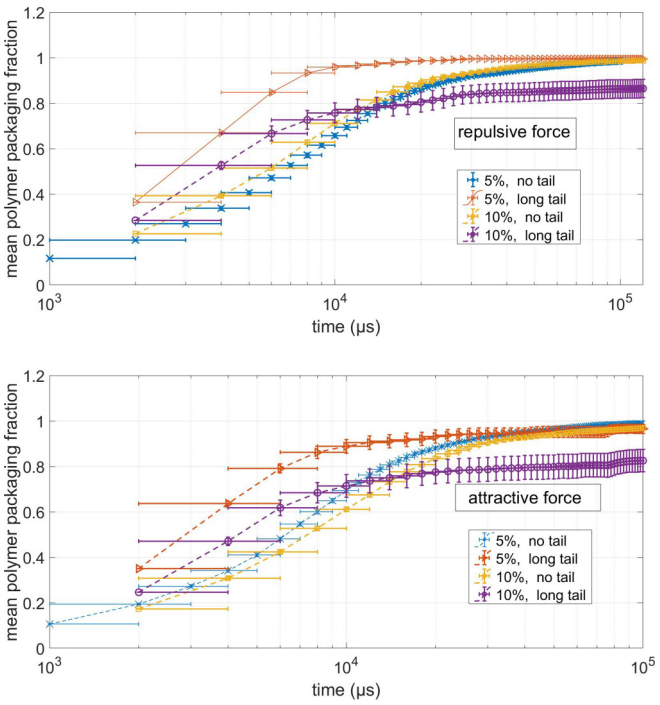

FIG. 6. The mean polymer packing fraction in a capsid versus time during packing a polymer into a capsid with and without a tail inside a cell containing 3000 proteins (5% volume fraction) and one containing 6000 proteins (10% volume fraction). (a) Interactions among all beads are repulsive. (b) Forces between proteins and viral polymer are attractive.

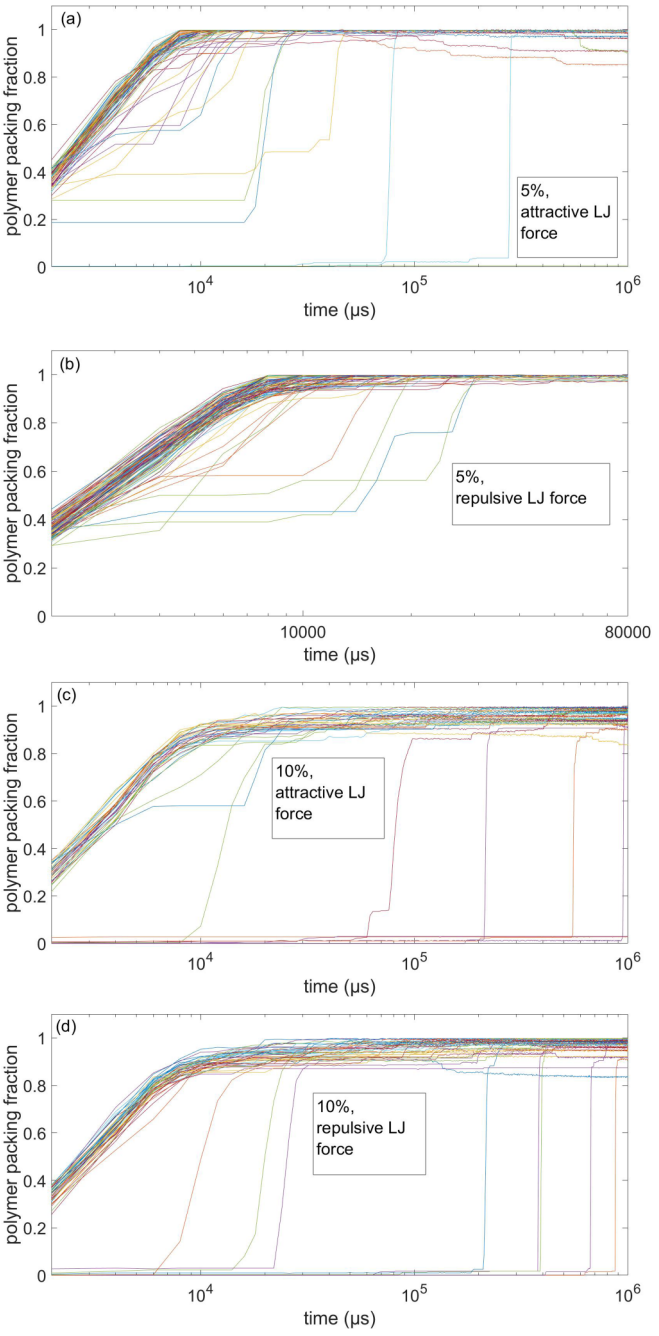

FIG. 7. Polymer length packing fraction from individual simulation runs versus time during packing into a capsid with a long tail under the presence of different number of protein beads. Proteins volume fractions are indicated in the figures.

packing into a capsid with a long tail [Fig. 3(b)], the effects of attractive and repulsive forces, within our statistics, are comparable in size.

Adding electrical interactions does not change the results significantly. Whether the electrical forces between the polymer and protein beads are attractive or repulsive, the packing rate is not affected much when compared to the case of packing a neutral polymer (Fig. 4). We have calculated the contribution of the elastic and electric energies to the packing process and find that at full packing the electrostatic forces contribute about 5% to the total energy while the elastic force contributes about 90%. As pointed out earlier, our apparent packing fraction of 0.34 bp/nm^3 is lower than what is reported elsewhere [37]. However, using the capsid internal volume, then our fraction 0.49 bp/nm^3 becomes more consistent with what is reported in the literature [29,37]. To check the effect of a packing fraction, we have performed more packing simulations with longer polymers of length 450 beads (the maximum we are able to pack in this study even with very large packing forces) inside a cell containing protein beads at 5% volume fraction. This gives a genome packing fraction of 0.4 bp/nm^3 if we use 25 nm as the capsid diameter, or 0.56 bp/nm^3 if we use the internal diameter of 22.5 nm. We do not see that electrical interactions make a difference. This result may reflect that most of the DNA charge is neutralized and is also highly screened under physiological conditions. (We have also performed simulations where the screening length is set to 1.9 nm, as in earlier studies [24], but we do not find much difference.) Our conclusions here are similar to what is found by Forrey and Muthukumar [26]. It should be noted that other theoretical calculations [29] and experiments [38] indicate that electrostatic forces can be significant. However, these studies have been performed reflecting specific *in vitro* experimental conditions. In addition, theoretical studies provide higher calculated packing forces close to full packing than what is found in some experiments (for example, measured forces at full packing level off at about 50 pN for ϕ29 [1], but rise sharply in theoretical calculations [29]).

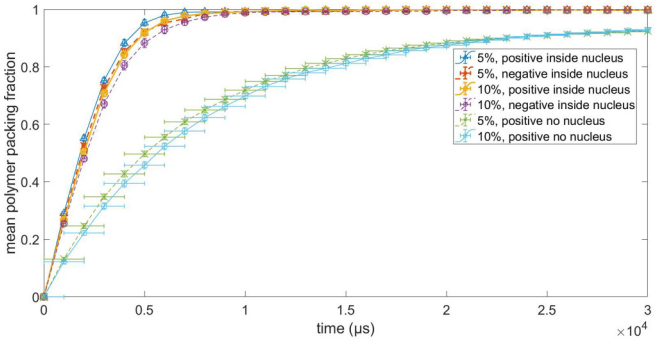

FIG. 8. The mean polymer length packing fraction in capsid with no tail versus time during packing the polymer from a nucleus into a tailless capsid inside a cell compared with packing from a crowded cell into a tailless capsid. Proteins volume fractions are indicated in the figure.

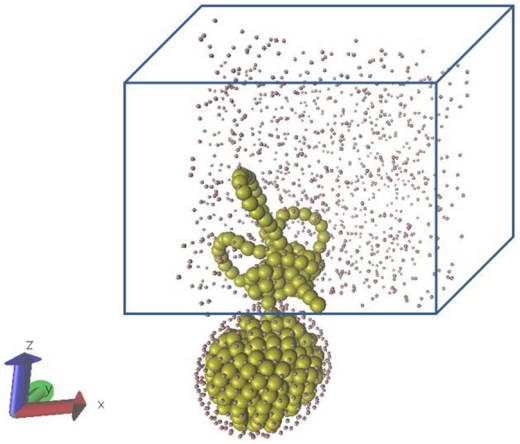

FIG. 9. Structure of packing semiflexible polymer from a nucleuslike structure that contains 1017 proteins into a tailless capsid. The size of protein beads is reduced to see the polymer more clearly.

C. Effect of capsid tail

Generally, the presence of the capsid tail makes it easier for a polymer to pack (Fig. 5), consistent with earlier work using a similar simulation model [24]. The effect is large (packing time is halved) due to the tail length. The polymer loses entropy when part of it is in the tail, making it easier to pack. Adding beads (5% volume fraction) that repel the polymer shows the same trend.

However, we see a reversal when 6000 beads (10% volume fraction) are present (Fig. 6). Initially, packing with a long tail is faster than with no tail. But the last 50–80 beads (0.1–0.2 μm) take a very long time to be packed into a capsid with a long tail, where stalling occurs. The presence of too many proteins adds frictional effects that make it more difficult for the motor, which is already working against the capsid pressure, to pack the last remaining beads of the polymer. This shows that at higher protein bead concentrations, some entropy is needed for the last remaining beads to fluctuate enough to find the tail entrance. It should be pointed out that the presence of the tail itself does not increase the protein beads concentration as its volume compared to that of the bacterial cell is less than a percent.

Some packing runs take time to initiate. We refer to this as the "waiting time" (Fig. 7). We define the waiting time as the time it takes to pack the initial 50 beads ($\sim$0.1 μm) of the polymer (protein beads interact repulsively with the polymer beads).

On the other hand, we do not see such large waiting times for packing into a tailless capsid. We also do not see this if we do not have protein beads in our simulations even if the tail is present. The waiting time clearly then results from the capsid tail, in which the polymers suffer entropic losses. The protein beads exert additional frictional drag on the polymer that makes it difficult for the polymer beads to be packed.

Furthermore, it can be seen in Fig. 7 that polymers in several simulations have exited the capsid after complete packing in almost one-third of the packing runs. This is seen in experiment by Shibata *et al.* [18] when ATP-γ-S is added. In our simulations, packing the polymer increases the internal capsid pressure causing the exit of the polymer.

D. Effect of nucleuslike structure

We incorporate in our simulations a small cubical cell, which contains protein beads, at the center of the bacterial cell to mimic packing of 201ϕ2-1 phage DNA inside a *P. chlororaphis* bacterium [Fig. 1(b)]. Figure 8 compares packing when the nucleus is present to the case where it is not. As seen earlier, electrical interactions do not play a major role in affecting the dynamics. However, we can see that the positive charges (5% and 10%) of proteins are slightly faster than the negative charges, which agree with the results found in the molecular study done by Cordoba *et al.* [25] that the existence of positive ions reduces the DNA-DNA electrostatic repulsion and speeds up the packing.

However, encapsulating the viral polymer by a nucleus greatly enhances packing, reducing packing time by a factor of 10 on average. This is because having the polymer inside a nucleus greatly reduces its configurational entropy, making it easier for the capsid motor to pack. Interestingly, knots are formed while packing is in progress (see Fig. 9 for a snapshot of one of the simulation runs). The knots are not formed during the equilibration phase, but form only when the motor pulls on the polymer for packing. The viral polymer is entangled with itself inside the nucleus at the end of equilibration. Then knots form once pulled from one end. Despite their presence, these knots quickly untangle and so do not hamper packing.

IV. CONCLUSION

In summary, we have investigated, through coarse-grained molecular dynamics simulations, the effects of cellular crowded environment on the packing process of a semiflexible polymer into a tailless capsid and into one with a long tail. Packing becomes more difficult at large volume fractions of the crowding particles, becoming slower if the interaction between crowding particle beads and polymer beads is attractive, since in this case the protein beads pull the polymer against the direction of the motor force.

At lower crowd particle volume fractions, and in contrast to packing into a tailless capsid, the waiting time before actual

packing ensues can be large for packing into a capsid with a tail. But once packing starts, the dynamics are faster than for a tailless capsid. At high crowding particle density, we find that packing into a capsid with a tail starts out faster than that into a tailless capsid. However, at later times, this reverses to the point that we see some polymer beads exiting the capsid. This is because frictional effects at higher volume fractions work with the capsid internal pressure to make packing more difficult.

It is interesting to note that in nature packing occurs with a tailless capsid for any known tailed phage; nature may have evolved in this direction for a more efficient process. Adding electrical interactions does not change the results significantly due to high viral DNA charge neutralization and screening.

Finally we have looked at the case of packing a polymer that is encapsulated by a nucleus. The entropic reduction offered by the nucleus increases packing speed, and may offer an explanation for its presence in some types of bacteria. Here, we have also observed knot formation, whose presence does not slow down the dynamics. These knots form due to pulling a confined polymer from one of its ends. It would be interesting to look at ejection *in vivo*, which is not well understood, and compare that with experiments. This is left for future work.

ACKNOWLEDGMENTS

We would like to thank Sultan Qaboos University for availing the High Performance Computing facility, which was used to perform the simulations for this work. We would also like to thank Prof. Davide Marenduzzo for hosting N.A.-N. in his group and for discussing the results of this work.

[1] D. E. Smith, S. J. Tans, S. B. Smith, S. Grimes, D. L. Anderson, and C. Bustamante, Nature (London) **413**, 6857 (2001).
[2] J. Kindt, S. Tzlil, A. Ben-Shaul, and W. M. Gelbart, Proc. Natl. Acad. Sci. USA **98**, 13671 (2001).
[3] D. Marenduzzo and C. Micheletti, J. Mol. Biol. **330**, 485 (2003).
[4] J. Arsuaga, R. K. Z. Tan, M. Vazquez, D. W. Sumners, and S. C. Harvey, Biophys. Chem. **101**, 475 (2002).
[5] J. C. LaMarque, T. L. Le, and S. C. Harvey, Biopolymers **73**, 348 (2003).
[6] P. K. Purohit, J. Kondev, and R. Phillips, J. Mech. Phys. Solids **51**, 2239 (2003).
[7] P. K. Purohit, J. Kondev, and R. Phillips, Proc. Natl. Acad. Sci. USA **100**, 3173 (2003).
[8] T. Odijk, Biophys. J. **75**, 1223 (1998).
[9] T. Odijk and F. Slok, J. Phys. Chem. B **107**, 8074 (2003).
[10] G. Zuccheri, A. Scipioni, V. Cavaliere, G. Gargiulo, P. De Santis, and B. Samori, Proc. Natl. Acad. Sci. USA **98**, 3074 (2001).
[11] R. F. Schleif and P. C. Wensink, *Practical Methods in Molecular Biology* (Springer-Verlag, New York, 1981).
[12] D. N. Fuller, D. M. Raymer, V. I. Kottadiel, V. B. Rao, and D. E. Smith, Proc. Natl. Acad. Sci. U.S.A. **104**, 16868 (2007).
[13] D. N. Fuller, D. M. Raymer, J. P. Rickgauer, R. M. Robertson, C. E. Catalano, D. L. Anderson, S. Grimes, and D. E. Smith, J. Mol. Biol. **373**, 1113 (2007).
[14] J. P. Rickgauer, D. N. Fuller, S. Grimes, P. J. Jardine, D. L. Anderson, and D. E. Smith, Biophys. J. **94**, 159 (2008).
[15] W. C. Earnshaw and S. C. Harrison, Nature (London) **268**, 598 (1977).
[16] M. E. Cerriteli, N. Chenq, A. H. Reosenberq, C. E. McPherson, F. P. Booy, and A. C. Steven, Cell **91**, 271 (1997).
[17] J. P. Mahalik, B. Hildebrandt, and M. Mithukumar, J. Biol. Phys. **39**, 229 (2013).
[18] H. Shibata, H. Fujisawat, and T. Minagawa, J. Mol. Biol. **196**, 845 (1987).
[19] M. Feiss, R. A. Fisher, M. A. Cryton, and C. Enger, Virology **77**, 281 (1977).
[20] V. Chaikeeratisak, K. Nguyen, K. Khanna, A. F. Brilot, M. L. Erb, J. K. C. Coker, A. Vavilina, G. L. Newton, R. Buschauer, K. Pogliano, E. Villa, D. A. Agard, and J. Pogliano, Science **355**, 194 (2017).
[21] I. Ali, D. Marenduzzo, and J. M. Yeomans, J. Chem. Phys. **121**, 8635 (2004).
[22] I. Ali, D. Marenduzzo, and J. M. Yeomans, Phys. Rev. Lett. **96**, 208102 (2006).
[23] D. Marenduzzo, Comput. Math. Methods Med. **9**, 317 (2008).
[24] A. Al-Lawati, I. Ali, and M. Al-Barawani, PLoS One **8**, 52958 (2013).
[25] A. Cordoba, D. M. Hinckly, J. Lequieu, and J. J. de Pablo, Biophys. J. **112**, 1302 (2017).
[26] C. Forrey and M. Muthukumar, Biophys. J. **99**, 25 (2006).
[27] C. Rebecca Locker, S. D. Fuller, and S. C. Harvey, Biophys. J. **93**, 2861 (2007).
[28] X. Agirrezabala, J. Martın-Benito, J. R. Casto, R. Miranda, J. M. Valpuesta, and J. L. Carrascosa, EMBO J. **24**, 3820 (2005).
[29] P. K. Purohit, M. M. Inamdar, P. D. Grayson, T. M. Squires, J. Kondev, and R. Phillips, Biophys. J. **88**, 851 (2005).
[30] See http://lammps.sandia.gov.
[31] Ji Youn Lim, J. W. Yoon, and C. J. Hovde, J. Microbiol. Biotechnol. **20**, 5 (2010).
[32] I. B. Powell, D. L. Tulloch, A. J. Hillier, and B. E. Davidson, J. Gen. Microbiol. **138**, 945 (1991).
[33] C. Svaneborg and R. Everaers, arXiv:1808.03503v1.
[34] S. W. Fetsko and P. T. Cummings, J. Rheol. **39**, 285 (1995).
[35] C. P. Broedersz and F. C. MacKintosh, Rev. Mod. Phys. **86**, 995 (2014).
[36] T. Ando and J. Skolnick, Proc. Natl. Acad. Sci. USA **107**, 18457 (2010).
[37] W. C. Earnshaw and S. R. Casjens, Cell **21**, 319 (1980).
[38] D. N. Fuller, J. P. Rickgauer, P. J. Jardine, S. Grimes, D. L. Anderson, and D. E. Smith, Proc. Natl. Acad. Sci. USA **104**, 11245 (2007).

[39] M. Joyeux, J. Phys.: Condens. Matter **27**, 383001 (2015).
[40] M. P. Allen and D. J. Tildesley, *Computer Simulation of Liquids* (Clarendon, Oxford, UK, 2017).
[41] Z. T. Berndsena, N. Kellera, S. Grimesc, P. J. Jardinec, and D. E. Smitha, Proc. Natl. Acad. Sci. USA **111**, 8345 (2014).
[42] C. Jeon, Y. Jung, and B.-Y. Ha, Soft Matter, **12**, 9436 (2016).
[43] I. J. Molineux, Mol. Microbiol. **40**, 1 (2001).